The results are plotted in Figs. 1–4 in the manner of Ref. 3 so as to facilitate comparison with the performance of other turbulence models discussed therein. The plots show the cross-stream distributions of U, k, and $-\overline{uv}$ expressed in wall units. The channel-flow results from the k-$\tilde{\varepsilon}$ model are identical to those obtained in Ref. 3. They show that the k-$\tilde{\varepsilon}$ model fails badly to predict the peak in k obtained from the simulations at $y^+ \approx 20$. The q-ζ model with the Launder–Sharma[8] functions performs a little better in this respect, whereas the use of the Chien functions in this model produces k^+ values generally greater than those of the simulations, also in accord with the findings of Ref. 3 for Chien's original model. Although the calculated $\overline{uv}^+$ distributions for the two channel flows agree closely with the DNS results, the mean velocity is rather too high in the logarithmic region. The discrepancy between the calculations and the DNS results is attributable to shortcomings in the viscous-damping functions employed. In this respect the q-ζ model gives typical results. The boundary-layer calculations exhibit broadly the same features; the chief difference being that the agreement with the simulated and measured shear-stress is not as good.

On the whole, the results obtained from the q-ζ models are in no way inferior to those obtained from the established k-$\tilde{\varepsilon}$ models considered. But they have been obtained with considerably less computational effort. The superior behavior of q and ζ in the sublayers permits the use of a relatively coarse grid (in the $\mathrm{Re}_\tau = 395$ channel-flow calculations, 30 cross-stream nodes instead of 40), and the omission of redundant source terms further reduces the computer time required. Grid-independent solutions for the low-Reynolds-number channel flow were obtained in 75% of the CPU time needed for the same calculations with the k-$\tilde{\varepsilon}$ model. The saving in CPU time is enhanced when the Reynolds number is increased, to approximately 50% for the boundary-layer calculations at $\mathrm{Re}_\vartheta = 5480$.

Conclusion

These first results are encouraging but a good deal more needs to be done. Further work should no doubt be concentrated on the formulation of new viscous-layer damping functions in the ζ equation, with special attention paid to the constraints imposed by the need for consistent boundary conditions at the wall. For the present calculations we have been content to borrow functions from established k-ε models as a temporary expedient. The present short paper is intended only to draw attention to the possibilities.

Acknowledgment

We gratefully acknowledge financial support for A. A. Dafa'Alla from the Engineering and Physical Sciences Research Council.

References

[1]Speziale, C. G., Abid, R., and Anderson, E. C., "Critical Evaluation of Two-Equation Models for Near-Wall Turbulence," *AIAA Journal*, Vol. 30, No. 2, 1992, pp. 324–331.

[2]Shih, T.-H., and Hsu, A. T., "An Improved k-ε Model for Near-Wall Turbulence," AIAA Paper 91-0611, 1991.

[3]Lang, N. J., and Shih, T.-H., "A Critical Comparison of Two-Equation Turbulence Models," NASA TM 105237, ICOMP-91-15, 1991.

[4]Rodi, W., and Mansour, N. N., "Low Reynolds Number k-ε Modelling with the Aid of Direct Simulation Data," *Journal of Fluid Mechanics*, Vol. 250, 1993, pp. 509–529.

[5]Spalding, D. B., "Kolmogorov's Two-Equation Model of Turbulence," *Proceedings of the Royal Society Ser. A*, Vol. 434, 1991, pp. 211–216.

[6]Jones, W. P., and Launder, B. E., "The Prediction of Laminarization with a Two-Equation Model of Turbulence," *International Journal of Heat and Mass Transfer*, Vol. 15, No. 2, 1972, pp. 301–313.

[7]Coakley, T. J., "Turbulence Modelling Methods for the Compressible Navier-Stokes Equations," AIAA Paper 83-1693, 1983.

[8]Launder, B. E., and Sharma, B. I., "Application of the Energy-Dissipation Model of Turbulence to the Calculation of the Flow near a Spinning Disk," *Letters in Heat and Mass Transfer*, Vol. 1, No. 1, 1974, pp. 131–138.

[9]Chien, K.-Y., "Predictions of Channel and Boundary Layer Flows with a Low-Reynolds-Number Turbulence Model," *AIAA Journal*, Vol. 20, No. 1, 1982, pp. 33–38.

[10]Mansour, N. N., Kim, J., and Moin, P., "Near-Wall k-ε Modeling," *AIAA Journal*, Vol. 27, No. 8, 1989, pp. 1068–1073.

[11]Kim, J., Moin, P., and Moser, R., "Turbulence Statistics in Fully Developed Channel Flow at Low Reynolds Number," *Journal of Fluid Mechanics*, Vol. 177, 1987, pp. 133–166.

[12]Spalart, P. R., "Direct Simulation of a Turbulent Boundary Layer up to $R_\vartheta = 1410$," *Journal of Fluid Mechanics*, Vol. 187, 1988, pp. 61–98.

[13]Gibson, M. M., Verriopoulos, C. A., and Vlachos, N. S., "Turbulent Boundary Layer on Mildly Curved Convex Surface: 1 Mean Flow and Turbulence Measurements," *Experiments in Fluids*, Vol. 2, No. 1, 1984, pp. 17–24.

Computation of Compression Ramp Flow with a Cross-Diffusion Modified k–ε Model

Byong Kuk Yoon* and Myung Kyoon Chung†
Korea Advanced Institute of Science and Technology, Taejon 305-701, Republic of Korea

Introduction

SINCE the advent of the standard k–ε model, it has been very widely accepted as a quite dependable turbulence model in engineering field. Numerous tests however, have revealed its shortcomings in predicting nonequilibrium flows, such as the shock-wave/turbulent boundary-layer interaction flow over a ramp. In contrast, the k–ω model of Wilcox[1] produces significantly better skin friction distribution than the k–ε model for such nonequilibrium flows. Wilcox[2] attributed the better performance of the k–ω model to a cross diffusion between k and ε implicitly contained in the ω equation; k and ε which determine the turbulence length scale near the wall under a nonnegligible pressure gradient are strongly interdependent on each other.

Actually, it was shown by Leslie[3] with a statistical analysis that the turbulent transport term in the k equation depends on both gradient diffusions of k and ε. However, it has not been fully examined whether the cross-diffusion term should indeed be included in the conventional k–ε model or not. This Note is aimed at proposing a new k–ε model with a cross-diffusion term that can be used to analyze turbulent nonequilibrium flows.

Model Equations

Most extensive turbulent diffusion models for k and ε equations have been derived by Yoshizawa[4] with the two-scale direct-interaction approximation (TSDIA) as follows:

$$T_k = \frac{\partial}{\partial x_j}\left(C_{kk}C_\mu \frac{k^2}{\varepsilon}\frac{\partial k}{\partial x_j}\right) + \frac{\partial}{\partial x_j}\left(C_k C_\mu \frac{k^3}{\varepsilon^2}\frac{\partial \varepsilon}{\partial x_j}\right) \tag{1}$$

$$T_\varepsilon = \frac{\partial}{\partial x_j}\left(C_{\varepsilon\varepsilon}C_\mu \frac{k^2}{\varepsilon}\frac{\partial \varepsilon}{\partial x_j}\right) + C_\mu\left[\frac{\partial}{\partial x_j}\left(C_{\varepsilon k} k \frac{\partial k}{\partial x_j}\right) + C'_{\varepsilon 1}\left(\frac{\partial k}{\partial x_j}\right)^2 + C'_{\varepsilon 2}\frac{k}{\varepsilon}\frac{\partial k}{\partial x_j}\frac{\partial \varepsilon}{\partial x_j} + C'_{\varepsilon 3}\frac{k^2}{\varepsilon^2}\left(\frac{\partial \varepsilon}{\partial x_j}\right)^2\right] \tag{2}$$

where C_{kk}, $C_{\varepsilon\varepsilon}$, $C_{k\varepsilon}$, $C_{\varepsilon k}$, $C'_{\varepsilon 1}$, $C'_{\varepsilon 2}$, and $C'_{\varepsilon 3}$ are model constants. Note that the conventional k–ε model adopts the first terms only in these models. Because of the plethora of the model constants, however, they have not been further pursued in practical applications.

Received Nov. 29, 1994; revision received March 14, 1995; accepted for publication March 14, 1995.

*Graduate Research Assistant, Department of Mechanical Engineering, Yusong-ku.

†Professor, Department of Mechanical Engineering, Yusong-ku.

When Wilcox[5] proposed the k–ω model, he showed that his ω equation is equivalent to the ε equation if a cross-diffusion term proportional to $(\partial k/\partial x_j)(\partial \omega/\partial x_j)$ is introduced into the standard ε equation. On expanding this term, one can see that the presence of such a cross-diffusion term is justified theoretically by TSDIA. Therefore, in order to improve the prediction capability of the k–ε model, a cross-diffusion term should be included as follows:

$$\frac{Dk}{Dt} = P_k - \varepsilon + \frac{\partial}{\partial x_j}\left[\frac{\nu_t}{\sigma_k}\frac{\partial k}{\partial x_j}\right] \tag{3}$$

$$\frac{D\varepsilon}{Dt} = C_{\varepsilon 1}\frac{\varepsilon}{k}P_k - C_{\varepsilon 2}\frac{\varepsilon^2}{k} + \frac{\partial}{\partial x_j}\left[\frac{\nu_t}{\sigma_\varepsilon}\frac{\partial \varepsilon}{\partial x_j}\right] + C_{\varepsilon 3}C_\mu \frac{k^3}{\varepsilon}\frac{\partial k}{\partial x_j}\frac{\partial}{\partial x_j}\left(\frac{\varepsilon}{k}\right) \tag{4}$$

To estimate the newly introduced constant $C_{\varepsilon 3}$, one applies the consistency condition that has been developed by Lele.[6] Lele solved a nonlinear diffusion-destruction equation that describes the propagation of turbulence properties produced by a planar source. As a consistency requirement, he postulated that the ε front must have the same propagation speed as the k front.

For one-dimensional incompressible flow at high-Reynolds number, Eq. (4) may be written as

$$\frac{\partial \varepsilon}{\partial t} - \beta\frac{\partial^2 \varepsilon}{\partial z^2} - \frac{\beta}{3}\left(\frac{1}{\phi}\frac{\partial \phi}{\partial z}\right)\frac{\partial \varepsilon}{\partial z} - \left[C_{\varepsilon 3}C_\mu \frac{\partial \phi^{\frac{2}{3}}}{\partial z}\frac{\partial}{\partial z}\left(\frac{\varepsilon}{\phi^{\frac{2}{3}}}\right)\right] + \psi\varepsilon = 0 \tag{5}$$

where $\beta = C_\mu/4\sigma_\varepsilon$, $\phi = (2k)^{3/2}$, and $\psi = 2C_{\varepsilon 2}$. Equation (5) is identical to the Eq. (14) in Ref. 6, except for the cross-diffusion term in the brackets. Applying the same procedure of Lele to Eq. (5) with a transformation $\varepsilon(z,t) = \exp[z(\beta + 2C_\mu C_{\varepsilon 3})/2\beta\sqrt{3\alpha}]\ \bar{\varepsilon}(z,t)$, one obtains the following consistency condition:

$$C_{\varepsilon 3} = \frac{1}{2}\left[-\frac{5}{\sigma_\varepsilon} + \sqrt{\frac{24}{\sigma_\varepsilon^2} - \frac{24C_{\varepsilon 2}}{\sigma_k\sigma_\varepsilon} + \frac{36}{\sigma_k^2}}\right] \tag{6}$$

Other constants of the proposed model may be readjusted by the asymptotic expansion method introduced by Takemitsu.[7] Now, consider series expansions of the turbulence properties near the wall region of a two-dimensional channel as follows:

$$\begin{aligned} \nu_t^* &= y^*\left(1 + a_1 y^* + a_2 y^{*2}\right) + \mathcal{O}(y^{*3}) \\ k^* &= 1 + b_1 y^* + b_2 y^{*2} + \mathcal{O}(y^{*3}) \\ \varepsilon^* &= \left[1 + c_1 y^* + c_2 y^{*2} + \mathcal{O}(y^{*3})\right]/y^* \end{aligned} \tag{7}$$

where $\nu_t^* = \nu_t/(Re\, u_\tau \kappa)$, $k^* = k/(u_\tau^2/\sqrt{C_\mu})$, $\varepsilon^* = \varepsilon/(u_\tau^3/\kappa)$, and $y^* = y/H$, and H is the channel height. Note that each leading term corresponds to the law of the wall.

Substituting Eqs. (7) into the governing equations for U, k, and ε in a fully developed incompressible channel flow,[7] one finds a_1, b_1, and c_1 as a function of the model constants,

$$a_1 = \left\{-2\cdot\left[3\left(\frac{C_{\varepsilon 2}}{C_{\varepsilon 1}} - 1\right) + \frac{\kappa^2}{\sigma_k\sqrt{C_\mu}}\right] - 2\frac{\kappa^2}{\sqrt{C_\mu}}\frac{C_{\varepsilon 3}}{C_{\varepsilon 1}}\right\}\Bigg/\left(\frac{C_{\varepsilon 2}}{C_{\varepsilon 1}} - 1\right)\left(2 - \frac{\kappa^2}{\sigma_k\sqrt{C_\mu}}\right) \tag{8a}$$

$$b_1 = -4\Bigg/\left(2 - \frac{\kappa^2}{\sigma_k\sqrt{C_\mu}}\right) \tag{8b}$$

$$c_1 = 2b_1 - a_1 \tag{8c}$$

From the zeroth-order solution of the ε equation, one obtains the following relation that is well known for local equilibrium flows with a logarithmic velocity distribution:

$$C_{\varepsilon 1} = C_{\varepsilon 2} - \kappa^2/\sigma_\varepsilon\sqrt{C_\mu} \tag{9}$$

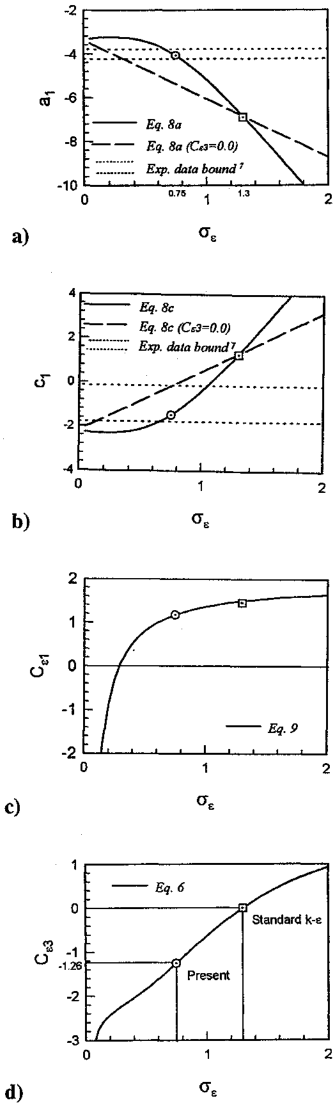

Fig. 1 Dependence of model constants a_1, c_1, $C_{\varepsilon 1}$, and $C_{\varepsilon 3}$ on σ_ε.

By substituting the constants of the standard k–ε model and the transformed k–ω model into Eqs. (8) and (9), the following tabulated values of a_1, b_1, c_1, and κ are obtained:

Experimental data[7]:

$\kappa \approx 0.41$, $a_1 \approx -4.2 \sim -3.8$, $b_1 \approx -2.8 \sim -2.2$

$c_1 \approx -1.8 \sim -0.1$

Standard k–ε model:

$\kappa \approx 0.43$, $a_1 \approx -7.1$, $b_1 \approx -2.9$, $c_1 \approx 1.3$

Transformed k–ω model:

$\kappa \approx 0.41$, $a_1 \approx -3.0$, $b_1 \approx -2.3$, $c_1 \approx -1.7$

Comparing them with the experimental values, it is found that the constants of the k–ω model produce much better near-wall variations of ν_t, k, and ε than those of the k–ε model. Especially, c_1 by the k–ε model has the sign opposite to the experimental data. On the basis of this result, the constants appearing in the proposed two-equation model, Eqs. (3) and (4), are determined in the following manner.

First, well-established empirical constants are retained in this model; $C_{\varepsilon 2} = 1.92$, $\kappa = 0.41$, and $\sigma_k = 1.0$. Substituting these constants into Eq. (6), one finds the constants a_1, c_1, $C_{\varepsilon 3}$, and $C_{\varepsilon 1}$ as functions of σ_ε, which are displayed in Figs. 1a–1d.

In Figs. 1a and 1b, the dashed curves represent those of the standard k–ε model where $C_{\varepsilon 3} = 0.0$. With the conventional value $\sigma_\varepsilon = 1.3$, the resulting a_1 and c_1 are too far out from the bounded range of the experimental data. From these two figures, the most appropriate value of σ_ε turns out to be $\sigma_\varepsilon = 0.75$. Consequently the remaining constants can be determined from either Eqs. (9) and (6) or Figs. 1c and 1d as $C_{\varepsilon 1} = 1.17$ and $C_{\varepsilon 3} = -1.26$.

In order to test the proposed model against wall-bounded flows, the near-wall terms in the Launder–Sharma[8] low-Reynolds number pointwise model are used in the following section.

Applications

To investigate the performance of the proposed model, it is applied to a two-dimensional channel flow and compression flows over 20- and 24-deg ramps.

Fully Developed Channel Flow

The first case corresponds to the turbulent flow in a plane channel at $Re_H = 5400$. The calculated profiles by the present cross-diffusion modified k–ε model, Launder–Sharma (LS) k–ε model and Wilcox k–ω model are compared with direct numerical simulation (DNS) data[9] in Fig. 2. It can be seen that the proposed model predicts the best eddy viscosity profile among the three models. Also in Fig. 2b, the LS model overpredicts the velocities in the outer layer, whereas the k–ω model underpredicts them. From this test computation, the model constants of the proposed k–ε model are found to have been properly selected for this simple two-dimensional channel flow.

Ramp Flow

The flow configuration selected for computation is that of the compression ramp flows measured by Settles et al.[10] To thoroughly compare the model performances, the flow solver[11] with the Yee's third-order MUSCL type total variation diminishing (TVD) scheme was used. The numbers of computational grids are 100×80 for the 20-deg ramp and 100×60 for the 24-deg ramp which were generated by using an elliptic grid generation technique. On the 20-deg ramp, the maximum y^+ at the first grid cell is 0.29 and on the 24-deg ramp the maximum y^+ at the first cell is 0.62. Figure 3 shows comparisons of the computed and the measured surface pressure distributions and skin friction distributions for the 20-deg and 24-deg ramps. The computations employing the LS model and the proposed model predict the overall pressure rise and the location of the onset of pressure rise reasonably well. Therefore, the surface pressure is insensitive to the cross-diffusion term. That is, the proposed cross-diffusion term has not any effect on the overall feature of the flowfield. In contrast, the prediction of skin frictions is dramatically improved by including the cross-diffusion term in the k–ε model; the computed values are lowered by about 30 $\sim$ 50% downstream of the reattachment point. Based on these results, the cross-diffusion term that admits the correct asymptotic variations of ν_t and ε near the wall is important to predict the reattached turbulent

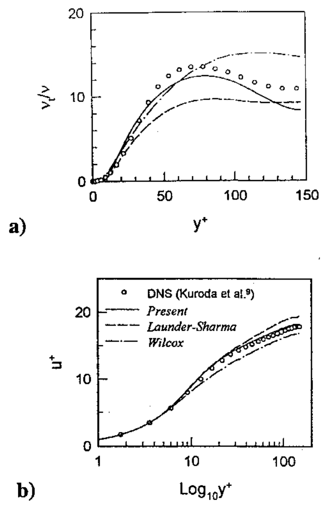

Fig. 2 Comparisons between DNS data and the predictions of eddy viscosity and mean velocity profiles in an incompressible channel flow.

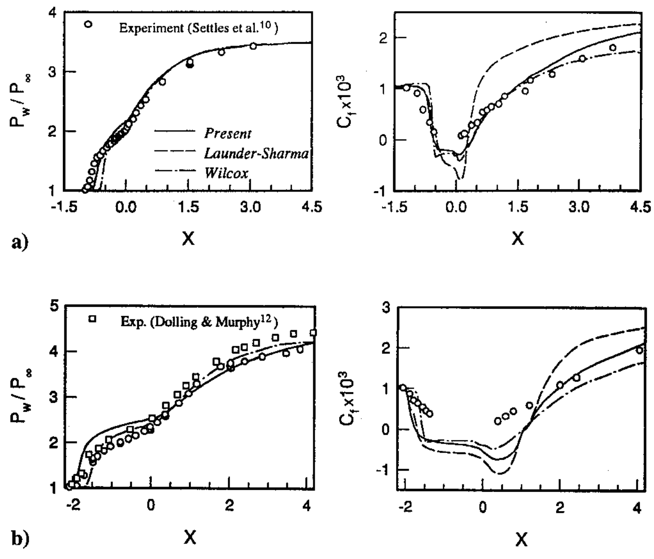

Fig. 3 Surface pressure distributions and skin friction coefficients in compression ramp flows: α = a) 20 deg and b) 24 deg.

boundary layers. Care must be taken, however, when the proposed ε equation modified by the cross diffusion is extended for computations of free shear flow. It may lead to the same problem as that of the k–ω model in that the predictions are sensitive to the computational boundary value ω_∞.

Conclusions

Through comparison of the diffusion terms in the k–ε model, the k–ω model and Yoshizawa's statistical model,[4] we realized that the cross-diffusion terms are essential in the k–ε model. The set of model constants in the present cross-diffusion modified k–ε model has been determined based on the near-wall behavior of turbulence and a consistency condition. The two-dimensional channel flow was best computed by the proposed model, and it was found that the cross-diffusion term plays a decisive role in the prediction of skin friction in nonequilibrium flows such as shock-wave/turbulent-boundary-layer interaction flow over a ramp.

References

[1] Wilcox, D. C., "Supersonic Compression-Corner Applications of a Multiscale Model for Turbulent Flows," *AIAA Journal*, Vol. 28, No. 7, 1990, pp. 1194–1198.

[2] Wilcox, D. C., "Turbulence Modeling for CFD," DCW Industries, Inc., La Cañada, CA, 1993.

[3] Leslie, D. C., *Developments in the Theory of Turbulence*, Clarendon, Oxford, England, UK, 1973. pp. 335–342.

[4] Yoshizawa, A., "Statistical Modeling of a Transport Equation for the Kinetic Energy Dissipation Rate," *Physics of Fluids A*, Vol. 30, No. 3, 1987, pp. 628–631.

[5] Wilcox, D. C., "Reassessment of the Scale-Determining Equation for Advanced Turbulence Models," *AIAA Journal*, Vol. 26, No. 11, 1988, pp. 1299–1310.

[6] Lele, S. K., "A Consistency Condition for Reynolds Stress Closures," *Physics of Fluids A*, Vol. 28, No. 1, 1987, pp. 64–68.

[7] Takemitsu, N., "An Analytical Study of the Standard k–ε Model," *Journal of Fluids Engineering*, Vol. 112, No. 2, 1990, pp. 192–198.

[8] Launder, B. E., and Sharma, B. I., "Application of the Energy Dissipation Model of Turbulence to the Calculation of Flows near a Spinning Disk," *Letters in Heat and Mass Transfer*, Vol. 1, 1974, pp. 131–138.

[9] Kuroda, A., Kasagi, N., and Hirata, M., "A Direct Numerical Simulation of the Turbulent Flow Between Two Parallel Walls: Turbulence Characteristics Near the Wall Without Mean Shear," *5th Symposium on Numerical Simulation of Turbulence*, Inst. of Industrial Science of the Univ. of Tokyo, 1990, pp. 1–5.

[10] Settles, G. S., Fitzpatrick, T. J., and Bogdonoff, S. M., "Detailed Study of Attached and Separated Compression Corner Flow Fields in High Reynolds Number Supersonic Flow," *AIAA Journal*, Vol. 17, No. 6, 1979, pp. 579–585.

[11] Yoon, B. K., Chung, M. K., and Park, S. O., "A Computational Study on Shock-Wave/Turbulent-Boundary-Layer Interaction with Two-Equation Turbulence Models," AIAA Paper 94-2276, June 1994.

[12]Dolling, D. S., and Murphy, M. T., "Unsteadiness of the Separation Shock Wave Structure in a Supersonic Compression Ramp Flowfield," *AIAA Journal*, Vol. 21, No. 12, 1983, pp. 1628–1634.

Active Control of Boundary-Layer Instabilities: Use of Sensors and Spectral Controller

R. D. Joslin,* R. A. Nicolaides,† G. Erlebacher,‡
M. Y. Hussaini,§ and M. D. Gunzburger¶
NASA Langley Research Center, Hampton, Virginia 23681-0001

Introduction

THIS second study focuses on the suppression of instability growth using an automated active-control technique. This automated approach is the next logical step based on previous experimental and computational studies reviewed by Joslin et al.[1] and Thomas,[2] in which the control was in the form of wave cancellation. The wave-cancellation method assumes that a wavelike disturbance can be linearly canceled by introducing another wave that has a similar amplitude but that differs in phase. Both experimental and computational results have demonstrated that two-dimensional Tollmien–Schlichting (TS) waves can be superposed upon two-dimensional waves in such a way as to reduce the amplitudes in the original waves under the presumption of wave cancellation. Joslin et al.[1] have definitively shown that flow control by wave cancellation is the mechanism for the observed phenomena. Three simulations were performed in their computational study to demonstrate the wave-cancellation concept. The first simulation obtained the evolution of a two-dimensional instability generated by periodic suction and blowing forcing, the second simulation yielded an instability caused by a suction and blowing actuator in the absence of and downstream of the forcing used in the first simulation, and the third simulation computed the evolution of a disturbance resulting from both forcing and actuator suction and blowing (wave-cancellation test case). Joslin et al.[1] showed that the superposition of the first and second simulation results exactly matched the wave-cancellation simulation results.

Based on the wave-cancellation assumption, the evolution and automated control of spatially growing two-dimensional disturbances in a flat-plate boundary layer are computed. Although the present active-control approach is demonstrated here for a two-dimensional instability test case, the ultimate goal of this line of research is to introduce automated control to external flow over an actual aircraft or to any flow that has instabilities that require suppression.

The nonlinear computations consist of the integration of the sensors, actuators, and controller as follows: the sensors will record the unsteady pressure or shear on the wall; the spectral analyzer (controller) will analyze the sensor data and prescribe a rational output signal; the actuator will use this output signal to control the disturbance growth and stabilize the instabilities within the laminar boundary layer. This scenario is shown in Fig. 1. Although a closed-loop feedback system could be implemented (using an additional sensor downstream of the actuator) to fully automate the control and to lead to an exact cancellation of the instability, the feedback will not be introduced here due to the added computational expense of the iterative procedure.

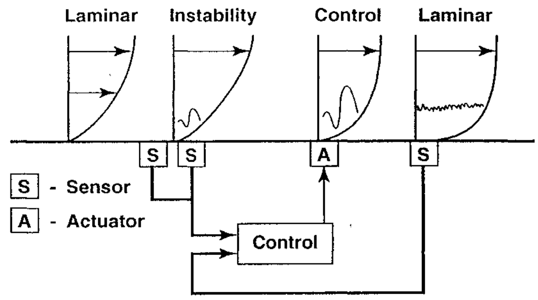

Fig. 1 Schematic of active control with wave cancellation.

Numerical Techniques

The nonlinear, unsteady Navier–Stokes equations are solved by direct numerical simulation (DNS) of disturbances, which evolve spatially within the boundary layer. The spatial DNS[3,4] approach involves spectral and high-order finite difference methods and a three-stage Runge–Kutta method[5] for time advancement. The influence-matrix technique is employed to solve the resulting pressure equation.[6,7] Disturbances are forced into the boundary layer by unsteady suction and blowing through a slot in the wall. At the outflow boundary, the buffer-domain technique of Streett and Macaraeg[8] is used.

The equations are nondimensionalized with the freestream velocity U_∞, the kinematic viscosity ν, and the inflow displacement thickness δ_0^*. The Reynolds number becomes $R = U_\infty \delta_0^*/\nu$, and the frequency is $\omega = \omega^* \delta_0^*/U_\infty$.

Control Method

Here, the term "controller" refers to the logic that is used to translate sensor-supplied data into a response for the actuator, based on some control law. For the present study, a spectral controller requires a knowledge of the distribution of energy over frequencies and spatial wave numbers. For this automated controller system, a minimum of two sensors must be used to record either the unsteady pressure or unsteady shear at the wall. By using Fourier theory, this unsteady data can be transformed via

$$f(\omega) = \int_{-\infty}^{\infty} f(t) e^{-i\omega t}\, \mathrm{d}t \tag{1}$$

where $f(t)$ is the signal and ω is the frequency. This transform yields an energy spectrum that indicates which frequencies exist in the signal and how much relative energy each frequency contains.

The largest Fourier coefficient indicates the frequency that will be used to control the instability, although the largest growth rate can be used instead of largest coefficient. The information from the two sensors is used to obtain estimates of both spatial growth rates and phase via the relation

$$\alpha = \frac{1}{A}\frac{\mathrm{d}A}{\mathrm{d}x} \tag{2}$$

This temporal and spatial information is then substituted into the assumed control law, or wall-normal velocity boundary condition,

$$v_s(x, t) = v_w \times p_w^1 \exp\left[i(\omega + \phi_t)t + \alpha x_s\right] + \text{c.c.} \tag{3}$$

where p_w^1 is the complex pressure (or shear) for the dominant frequency mode (or largest growth-rate mode) at the first sensor, ω is the dominant mode determined from Eq. (1), ϕ_t is the phase

Received Nov. 26, 1994; revision received Jan. 31, 1995; accepted for publication Jan. 31, 1995.

*Research Engineer, Fluid Mechanics and Acoustics Division. Member AIAA.

†Consultant, Institute for Computer Applications in Science and Engineering; currently Professor, Department of Mathematics, Carnegie Mellon University, Pittsburgh, PA 15213.

‡Research Fellow, Institute for Computer Applications in Science and Engineering. Member AIAA.

§Director, Institute for Computer Applications in Science and Engineering. Member AIAA.

¶Consultant, Institute for Computer Applications in Science and Engineering; currently Professor, Department of Mathematics, Virginia Polytechnic Institute and State University, Blacksburg, VA 24061.